Robust Surface Remeshing Based on Conformal Welding

Wei Chen* Siquan Sun† Yue Wang† Na Lei‡ Chander Sadasivan †
Apostolos Tassiopoulos† Shikui Chen† Hang Si§ Xianfeng Gu†

Abstract

This work proposes a novel algorithm to eliminate the self-overlapping based on conformal welding theory, to improve the robustness of the surface remeshing algorithm. The proposed algorithm constructs a planar annulus with a high-quality triangulation, then weld the input surface with the annulus along their corresponding boundary components. The welded surface has a well-defined Riemannian metric and can be conformally mapped onto a convex planar domain by using the dynamic discrete surface Ricci flow method. This method guarantees the conformal mapping restricted on the input surface is a global embedding, and resolves the problem of self-intersections in the neighborhood of the boundary. The conformal welding method has been tested to remesh real car models. The experimental results demonstrate the method is highly effective in practice and greatly improves the robustness of the remeshing algorithm based on conformal uniformization.

1 Introduction

Surface mesh generation plays a fundamental role in CAD/CAE fields. Planar mesh generation methods are relatively mature, such as the Delaunay refinement method [2], and the centroidal Voronoi diagram method [6]. Surface meshing is much more challenging.

Recently, Si et. al. [15] introduced a novel algorithm for generating high quality triangulations on surfaces with complicated topologies based on conformal uniformization. The original CAD model is converted to a low-quality triangle mesh, obtained by triangulation on the parameter domain and refined by necessary preprocessing steps, such that the mesh is a water-tight manifold. The key idea is to flatten the input triangle mesh onto a planar domain by an angle-preserving (conformal) map, then a high quality planar mesh is generated and pulled back to the 3D surface. Since the mapping is angle-preserving, the Delaunay property is preserved in the surface triangulation. Furthermore, the planar sampling density is adaptive to the surface area element and the curvature, this ensures the surface meshing quality. Fig. 1 shows one example of remeshing a car chassis model based on conformal uniformization: frame (a) shows the 3D car chassis model; frame (b) illustrates the surface is flattened by a conformal mapping; frame (c) demonstrates the conformality of the mapping by checkerboard texture mapping, all the right corner angles of the checkers are well preserved; the planar image is triangulated using Delaunay refinement algorithm, the pull back triangulation on the surface has high qualities as shown in frame (d).

In most scenarios, the quality of the input triangle mesh is often low, posing a significant risk to the stability and convergence of standard conformal mapping algorithms. We choose the dynamic surface Ricci flow method [11, 10] to compute the parameterization because it has a theoretic guarantee to produce the unique Riemannian metric, conformal to the initial metric and inducing the prescribed curvature. Furthermore, dynamic surface Ricci flow is capable of handling low-quality input meshes and automatically improves the triangulation to remain Delaunay with final Riemannian metric.

However, the parameterization result depends on the input geometry and the target curvature, it is possible that the final mapping is only a local embedding, namely the mapping restricted to the neighborhood of each vertex is injective and surjective, but globally the image of the whole input mesh may have self-intersections. Especially, if the surface has concave boundaries, the image of the neighborhood of the boundary may have overlaps. This causes great difficulties for the downstream planar Delaunay refinement algorithm. As shown in Fig. 2, frame (a) shows a shield of a car tire model, frame (b) illustrates the conformal parameterization result, and the self-intersections can be found in the neighborhood of the boundary.

To tackle this challenge, this work proposes a novel algorithm to improve the robustness of surface remeshing based on conformal welding technnique [9, 17]. Suppose the input surface M is a topological poly-annulus, namely a genus zero surface with multiple boundary components $\{\gamma_1, \ldots, \gamma_k\}$, We can seamlessly merge M with a topological annulus A having boundaries τ_1 and τ_2, aligning them correspondingly with γ_1 and τ_1, $\varphi : \gamma_1 \to \tau_1$. The merged surface $S \leftarrow M \cup_\varphi A$ is a topo-

*Capital Normal University.
†Stony Brook University.
‡Corresponding author, nalei@dlut.edu.cn, Dalian University of Technology.
§Cadence Design Systems Inc.

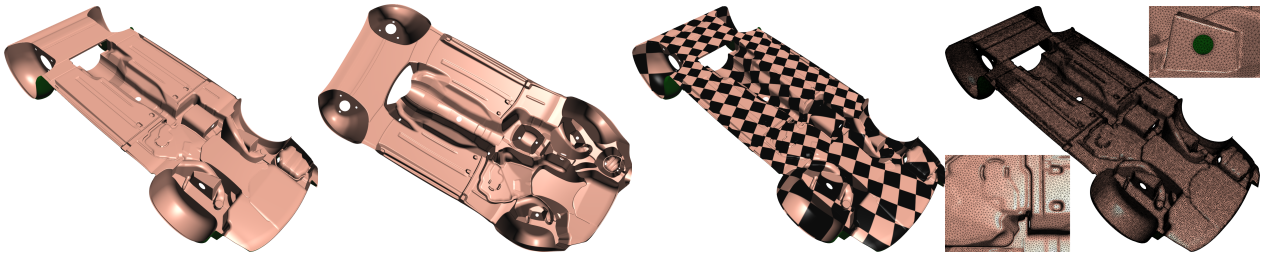

(a) 3D chassis model (b) conformal flattening (c) texture mapping (d) remeshing result

Figure 1: Remeshing a whole car chassis model based on conformal uniformization.

logical poly-annulus having boundaries $\tau_2, \gamma_2, \ldots, \gamma_n$. We treat τ_2 as the exterior boundary component, and $\gamma_2, \ldots, \gamma_n$ as the interior boundary components, and use the dynamic Ricci flow to map S onto a planar domain, such that the image of the exterior boundary τ_2 is convex (or nearly convex), so the mapping is an embedding, the input surface M is conformally flattened without any self-intersection. This *conformal welding* technique can greatly improve the robustness of the algorithm. As shown in Fig. 2, the input surface is welded with a topological annulus and the welded surface is conformally flattened in frame (c), the mapping restricted to the input surface has no overlap. Frame (d) shows conformality of the parameterization by checkerboard texture mapping.

1.1 Contribution This work proposes a novel algorithm to improve the robustness of surface remeshing based on conformal welding method. Suppose the input surface is a poly-annulus, we construct a topological cylinder with high quality triangulation and weld the input surface with the annulus along one boundary loop. By using dynamic discrete surface Ricci flow, the welded surface is conformally flattened onto a near convex domain on the plane. This method guarantees the conformal mapping restricted to the input surface is an embedding, and resolves the problem of self-intersections in the neighborhood of the boundary. In our experiments, we use the conformal welding method to remesh real car models, which shows the method is rigorous and practical, and significantly improves the robustness of the remeshing algorithm.

2 Previous Work

The objective of surface triangle mesh generation is to tessellate a given 3D surface into triangles, creating a discrete representation suitable for various applications, such as finite element analysis. Over the years, researchers have developed numerous algorithms and methods to address this challenge efficiently and accurately. This literature review highlights some prominent contributions in the field.

Delaunay-Based Approaches Delaunay triangulation is a widely used technique for surface mesh generation [2]. Shewchuk's Triangle [22] is a popular tool for computing Delaunay triangulations of planar straight-line graphs and is often used as a building block in surface meshing algorithms. In 3D, adaptive refinement techniques, such as Bowyer-Watson and incremental insertion [3], are employed to generate high-quality triangle meshes from point clouds or surfaces. Centroidal voronoi tessellation is also a popular method for high quality planar mesh generation [6].

Constrained Delaunay Triangulation Handling constraints, such as sharp edges and features, is crucial in surface meshing. Recent developments include the CGAL library, which provides efficient algorithms for constrained Delaunay triangulation and mesh generation [20]. These advancements enable the preservation of geometric features in the generated meshes.

Surface Reconstruction Methods Surface reconstruction aims to recover a continuous surface from point clouds or scattered data. Poisson surface reconstruction [16] is a notable technique that combines surface reconstruction and mesh generation. It leverages the Poisson equation to create a smooth surface representation and subsequently generates triangle meshes.

Variational Approaches Variational methods, such as surface fairing and optimization-based meshing, have gained attention. Garland and Heckbert's surface simplification algorithm [8] is a classic example. It iteratively collapses edges to create simplified triangle meshes while preserving important geometric characteristics.

Multi-resolution Techniques Multi-resolution representations are valuable for adaptive meshing.

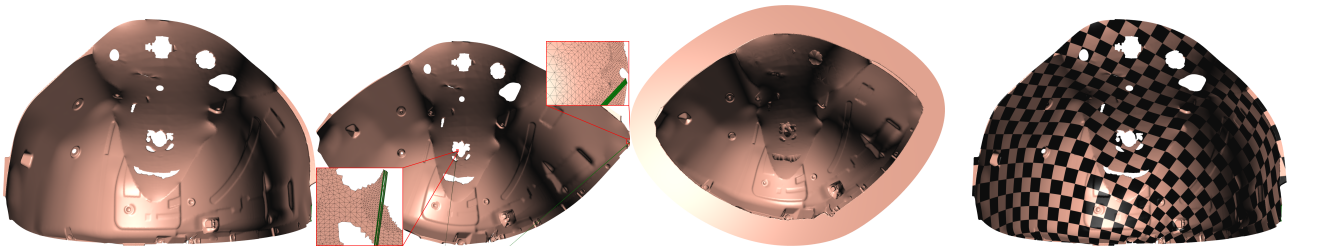

(a). wheel housing model (b). conformal flattening with self intersections (c). conformal flattening of the welded model (d). conformal texture mapping

Figure 2: Robust conformal parameterization of a shield of the car tire model. The conformal welding method eliminates the self-intersections.

The work of Alliez et al. on Progressive Meshes [1] introduced a framework for constructing levels of detail in triangle meshes. This concept has applications in real-time graphics and efficient transmission of 3D models.

Conformal Uniformization Based Method Recently, Si et. al. [15] introduced a novel algorithm for generating high quality triangulations on surfaces with complicated topologies based on conformal uniformization. The key idea is to flatten the input surface onto a planar domain by an angle-preserving (conformal) map, then a high quality planar mesh is generated and pulled back to the 3D surface. Since the mapping is angle-preserving, the Delaunay property is preserved to the surface triangulation. Furthermore, the planar sampling density is adaptive to the surface area element and the curvature, this guarantees the surface meshing quality.

However, for surfaces with complicated topologies, conformal parameterization algorithms can only guarantee the mapping is locally embedding, and globally immersion. Namely, they may produce self-intersections for concave boundary images. This will cause intrinsic difficulty for the planar Delaunay refinement algorithm since it always assumes the input has no self overlapping. The current work proposes to use the conformal welding method to glue the input surface with a topological annulus and map the glued surface onto a planar domain with convex boundary condition so that the restriction of the mapping on the initial surface is injective. This will greatly improve the robustness of the remeshing algorithm.

3 Theoretic Foundation

This section briefly introduces the theoretic background for surface conformal geometry and surface Ricci flow. For more details, we refer readers to [12, 13, 11, 10] for more thorough treatments.

3.1 Riemann Surface

Definition 3.0.1. (Holomorphic Function) *A complex function $f : \mathbb{C} \to \mathbb{C}$, $f(x+iy) = u+iv$, satisfies the following Cauchy-Riemann equation*

$$\frac{\partial u}{\partial x} = \frac{\partial v}{\partial y}, \quad \frac{\partial u}{\partial y} = -\frac{\partial v}{\partial x},$$

then f is called a holomorphic function. *If the inverse function f^{-1} exists and is also holomorphic, then f is called a* bi-holomorphic function.

Given a topological surface S with an atlas $\mathcal{A} = \{(U_\alpha, \varphi_\alpha)\}$, where U_α is an open set, $\varphi_\alpha : U_\alpha \to \mathbb{C}$ is a homeomorphism, $(U_\alpha, \varphi_\alpha)$ is a *local chart.* if $U_\alpha \cap U_\beta \neq \emptyset$, then the *transition map* is defined as

$$\varphi_{\alpha\beta} : \varphi_\alpha(U_\alpha \cap U_\beta) \to \varphi_\beta(U_\alpha \cap U_\beta), \varphi_{\alpha\beta} = \varphi_\beta \circ \varphi_\alpha.$$

If all the transition maps are bi-holomorphic, then $\mathcal{A}$ is called a *conformal structure.*

Definition 3.0.2. (Riemann Surface) *A topological surface with a conformal structure is called a* Riemann surface.

Definition 3.0.3. (Isothermal parameter) *Suppose $(S, \mathbf{g})$ is an oriented metric surface, and U is a neighborhood $U \subset S$ with the local coordinates (u, v)), such that the Riemannian metric has a special form*

$$\mathbf{g}(u, v) = e^{2\lambda(u,v)}(du^2 + dv^2),$$

then (u, v) are called the isothermal parameter *on U and $\lambda : U \to \mathbb{R}$ is called the* conformal factor *function.*

According to classicial surface differential geometry, for any point $p \in S$, one can always find an neighborhood of p, U_p, such that on U_p, one can define isothermal

coordinates $\varphi_p : U_p \to \mathbb{C}$. The union of isothermal coordinate charts $\{(U_p, \varphi_p)\}$ form a conformal structure, hence S is a Riemann surface.

Under the isothermal parameter, the Gaussian curvature of the surface can be computed as

$$K(x,y) = -\Delta_{\mathbf{g}}\lambda(x,y) = -\frac{1}{e^{2\lambda(x,y)}}\Delta\lambda(x,y).$$

The total Gaussian curvature is a topological invariant.

THEOREM 3.1. (GAUSS-BONNET) *Suppose $(S, \mathbf{g})$ is surface with a Riemannia metric, then*

$$\int_S KdA + \int_{\partial S} k_g ds = 2\pi\chi(S),$$

where $\chi(S)$ is the Euler characteristic number of S.

3.2 Smooth Surface Ricci Flow

DEFINITION 3.1.1. (PULL BACK METRIC) *Suppose $(S, \mathbf{g})$ and $(T, \mathbf{h})$ are two surfaces with Riemannian metrics, the local parameters of them are (x, y) and (u, v) respectively. The local representation of the metric tensor $\mathbf{h}$ is*

$$\mathbf{h}(u,v) = \begin{pmatrix} h_{11} & h_{12} \\ h_{21} & h_{22} \end{pmatrix}(u,v)$$

A C^1 mapping $\varphi : S \to T$ has a local representation,

$$(x,y) \mapsto (u(x,y), v(x,y)).$$

The pull back metric on S induced by φ is defined as

$$\varphi^*\mathbf{h}(x,y) = D\varphi^T \mathbf{h} D\varphi,$$

where $D\varphi$ is the Jacobi matrix of the mapping φ. $\varphi^*\mathbf{h}$ has the local representation

$$\varphi^*\mathbf{h} = \begin{pmatrix} u_x & u_y \\ v_x & v_y \end{pmatrix}^T \begin{pmatrix} h_{11} & h_{12} \\ h_{21} & h_{22} \end{pmatrix} \begin{pmatrix} u_x & u_y \\ v_x & v_y \end{pmatrix}.$$

DEFINITION 3.1.2. (CONFORMAL MAPPING) *Suppose $(S, \mathbf{g})$ and $(T, \mathbf{h})$ are surfaces with Riemannian metrics. A C^1 mapping $\varphi : S \to T$ is conformal, if*

$$\varphi^*\mathbf{h} = e^{2\lambda}\mathbf{g}, \tag{3.1}$$

where λ is the conformal factor function, $\lambda : S \to \mathbb{R}$.

A conformal mapping between two surfaces preserves local shapes and angles.

Suppose we conformally deform the surface Riemannian metric, $\mathbf{g} \to \bar{\mathbf{g}} = e^{2\lambda}\mathbf{g}$, then the Gaussian curvature changes according to the Yamabe equation,

$$\bar{K} = \frac{1}{e^{2\lambda}}\left(K - \Delta_{\mathbf{g}}\lambda\right).$$

If we set $\bar{K}$ to be constant, then we obtain the famous Koebe-Poincaré uniformization theorem.

THEOREM 3.2. (KOEBE-POINCARÉ UNIFORMIZATION) *Suppose $(S, \mathbf{g})$ is an orientable closed surface, then there is a scalar function $\lambda : S \to \mathbb{R}$, such that $\bar{\mathbf{g}} = e^{2\lambda}\mathbf{g}$ induces constant Gaussian curvature $\bar{K}$, where $\bar{K}$ equals one of $\{+1, 0, -1\}$ according to $\chi(S) > 0$, $\chi(S) = 0$ and $\chi(S) < 0$.*

The constant curvature metric is called the *uniformization metric* of the surface. Yamabe equation can be solved using Hamilton's *Ricci flow*, which has been used for the proof of Poincaré's conjecture [18, 19].

DEFINITION 3.2.1. (HAMILTON'S RICCI FLOW) *Suppose $(S, \mathbf{g})$ is a closed orientable metric surface, the normalized Ricci flow is defined as*

$$\partial_t \mathbf{g}(p,t) = 2\left(\frac{2\pi\chi(S)}{A(0)} - K(p,t)\right)\mathbf{g}(p,t).$$

Hamilton [14] and Chow [5] proved the convergence of surface Ricci flow.

3.3 Discrete Surface Ricci Flow Smooth surface Ricci flow theory can be generalized to the discrete polyhedral surfaces. A smooth surfaces is approximated by a polyhedral surface S with vertex set V. We call (S, V) a *marked surface*. Given a marked surface, we can define different triangulations. A *discrete Riemannian metric* for a marked surface (S, V) with a triangulation T can be represented as edge lengths $d : E \to \mathbb{R}^+$, satisfying the triangle inequality, namely on each face $[v_i, v_j, v_k]$,

$$d(v_i, v_j) + d(v_j, v_k) > d(v_i, v_k).$$

The discrete Riemannian metric determines the corner angles, by the cosine law

$$\cos\theta_i^{jk} = \frac{d^2(v_i,v_j) + d^2(v_k,v_i) - d^2(v_j,v_k)}{2d(v_i,v_j)d(v_k,v_i)}. \tag{3.2}$$

where θ_i^{jk} is the corner angle at v_i in the face $[v_i, v_j, v_k]$. Fix a discrete Riemannian metric, there are many triangulations, among them, the *Delaunay triangulation* is highly preferred.

DEFINITION 3.2.2. (DELAUNAY TRIANGULATION) *Given a closed marked surface (S, V) with a discrete Riemannian metric d, a triangulation T is called Delaunay, if for any edge $[v_i, v_j]$ shared by two faces $[v_i, v_j, v_k]$ and $[v_j, v_i, v_l]$, the condition*

$$\theta_k^{ij} + \theta_l^{ji} \leq \pi \tag{3.3}$$

always holds.

Definition 3.2.3. (Edge Flip Operator) *Given a closed marked surface (S, V) with a discrete Riemannian metric d and a triangulation T, an edge $[v_i, v_j]$ shared by two faces $[v_i, v_j, v_k]$ and $[v_j, v_i, v_l]$. The edge flip operator swaps the edge $[v_i, v_j]$ to $[v_k, v_l]$, and changes the triangles to $[v_i, v_l, v_k]$ and $[v_j, v_k, v_l]$.*

It is well known that we can modify a triangulation to be Delaunay by a sequence edge flip operators, such that a diagonal, for which the sum of its opposite angles is greater than π, is replaced by another diagonal.

The *discrete Gaussian curvature* is defined as the angle deficit,

$$K(v_i) = \begin{cases} 2\pi - \sum_{jk} \theta_i^{jk} & v_i \notin \partial M \\ \pi - \sum_{jk} \theta_i^{jk} & v_i \in \partial M \end{cases} \tag{3.4}$$

The total discrete Gaussian curvature also satisfies the Gauss-Bonnet theorem,

$$\sum_{v_i \in \partial M} K(v_i) + \sum_{v_i \notin \partial M} K(v_i) = 2\pi\chi(M).$$

The conformal deformation is defined analogously

Definition 3.2.4. (Vertex Scaling) *Suppose $M = (V, E, F)$ is a triangulated polyhedral surface, with a discrete metric $d : E \to \mathbb{R}^+$. $\lambda : V \to \mathbb{R}$ is the discrete conformal factor function defined on the vertex set V, the vertex scaling operator is defined as follows:*

$$d(v_i, v_j) \mapsto e^{u_i} d(v_i, v_j) e^{u_j}, \quad \forall\ [v_i, v_j] \in E. \tag{3.5}$$

The discrete conformal equivalence can be defined as follows: suppose d and d' are two polyhedral metrics of the marked surface (S, V), if there exists a sequence of triangulations T_i's and discrete metrics d_i's,

$$T_1, T_2, \ldots, T_n, \quad d = d_1, d_2, \ldots, d_n = d',$$

such that

1. T_i is Delaunay with respect to d_i;
2. if $T_i \neq T_{i+1}$ then they differ by an edge flip and $d_i = d_{i+1}$;
3. if $d_i \neq d_{i+1}$ then they differ by a vertex scaling and $T_i = T_{i+1}$.

Definition 3.2.5. (Discrete Conformal) *Two triangulated polyhedral metrics d and d' on a closed marked surface (S, V) are discrete conformal, if they are related by a sequence of two types of moves: vertex scaling and edge flip preserving Delaunay property.*

The discrete surface Ricci flow is defined similar to the smooth one.

Definition 3.2.6. (Discrete Surface Ricci Flow) *Given a marked surface (S, V) with a polyhedral metric d and a triangulation T, suppose the target Gaussian curvature $\bar{K} : T \to \mathbb{R}$ is given, then the Ricci flow is defined as*

$$\frac{d\lambda(v_i, t)}{dt} = \bar{K}(v_i) - K(v_i, t),$$

during the flow, the triangulation is updated to preserve the Delaunay property.

The discrete surface Ricci flow is the gradient flow of the following convex Ricci energy:

$$E(\lambda) := \int^{\lambda} \sum_{i=1}^{n} (\bar{K}(v_i) - K(v_i)) d\lambda_i. \tag{3.6}$$

The Hessian matrix of the Ricci energy can be represented by the cotangent edge weight, for each edge $[v_i, v_j]$,

$$w_{ij} = \cot \theta_k^{ij} + \cot_l^{ji}, \tag{3.7}$$

and the Hessain matrix is $H = (h_{ij})$

$$h_{ij} = \begin{cases} \sum_{k \neq i} w_{ik} & i = j \\ -w_{ij} & i \neq j \end{cases} \tag{3.8}$$

The existence and the uniqueness of the solution to the discrete surface Ricci flow is shown in the following theorem, the detail of the proof is in [11].

Theorem 3.3. (Discrete Surface Flow [11]) *Given a polyhedral metric d on a closed marked surface (S, V), and target curvature $\bar{K} : V \to (-\infty, 2\pi)$, such that $\bar{K}$ satisfies the Gauss-Bonnet condition $\sum K(v) = 2\pi\chi(S)$, there is a $\bar{d}$ discrete conformal to d, and $\bar{d}$ realized the curvature $\bar{k}$. $\bar{d}$ is unique update to a scaling, and can be obtained by the discrete surface Ricci flow.*

3.4 Conformal Welding Suppose $(S_1, \mathbf{g}_1)$ and $(S_2, \mathbf{g}_2)$ are two oriented compact surfaces with Riemannian metrics. Suppose $\gamma_1 \subset \partial S_1$ is a connected component on the boundary of S_1, $\gamma_2 \subset \partial S_2$ a connected component on the boundary of S_2. Without loss of generality, we can assume the total lengths of γ_1 and γ_2 are equal, otherwise we can perform a scaling. Furthermore, γ_1 and γ_2 are smooth curves. Let $\varphi : \gamma_1 \to \gamma_2$ is an isometric map between the two loops. We weld the two surfaces using φ as follows: each point $p \in \gamma_1$ is equivalent to its image $\varphi(p) \in \gamma_2$, the glued surface is

$$S := S_1 \bigcup_{p \sim \varphi(p)} S_2.$$

Let $U_1(p)$ be a neighborhood of p, $\varphi_1 : U_1(p) \to \mathbb{D}^2$ be a local conformal chart mapping $U_1(p)$ to the upper half disk of $\mathbb{D}^2$; $U_2(p)$ be a neighborhood of $\varphi(p)$, $\varphi_2 : U_2(p) \to \mathbb{D}^2$ be a local conformal chart mapping $U_2(p)$ to the lower half disk of $\mathbb{D}^2$. φ maps $\gamma_1|_{U_1}$ to $\gamma_2|_{U_2}$. By Schwartz reflection principle, φ_1 and φ_2 can be glued to a conformal map from

$$\varphi_1 \cup \varphi_2 : U_1(p) \cup U_2(\varphi(p)) \to \mathbb{D}^2.$$

This means S is a Riemann surface with well defined conformal structure.

4 Computational Algorithms

4.1 Overview The algorithmic pipeline is illustrated in Fig. 3. For a complex surface, the initial step involves segmenting it into several parts, each constituting a topological disk with or without holes. In the second step, for every part, each hole is filled by simply adding a vertex at the midpoint of the hole and connecting it to the edges along the boundary; thereafter, conformal welding is performed. The third step employs the discrete surface Ricci flow algorithm to compute the parameterization of the welded surface, with subsequent recovery of all boundaries. In the fourth step, planar Delaunay refinement is applied to the parameterization domain of the surface. Finally, in the last step, the remeshing result on the planar domain is pulled back onto the surface to obtain the final result.

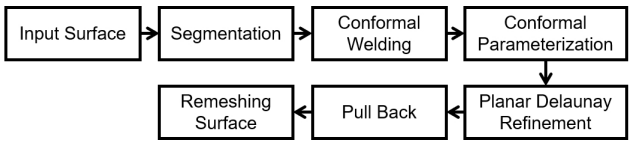

Figure 3: Pipeline of the algorithm.

4.2 Surface Segmentation Suppose the input surface is a genus g closed surface, we need to either manually or automatically decompose it into genus zero surface with multiple boundaries. This can be achieved using persistent homology method [7] to compute the handle loops and tunnel loops, and cut the surface along these loops. Another method is pants decomposition.

Given a triangle mesh M, we compute its Poincaré dual mesh $\bar{M}$, each vertex v, edge e and face f on M is dual to a face $\bar{v}$, edge $\bar{e}$ and vertex $\bar{f}$ on $\bar{M}$. We treat $\bar{M}$ as a graph of vertices and compute a spanning tree $\bar{T}$, then the *cut graph* Γ is defined as

$$\Gamma := \{e \in \mid \bar{e} \notin \bar{T}\}.$$

We slice M along Γ to obtain $\bar{M}$, for each vertex $v \in \Gamma$, there are $v^+, v^- \in \partial\bar{M}$, the shortest path $\bar{\gamma}$ on $\bar{M}$ corresponds to a loop γ on M. Furthermore, γ transversely intersects Γ, therefore γ is non-trivial in the homotopy group of the original mesh $\pi_1(M, p)$. We slice the surface along γ to reduce the topological complexity. By repeating this procedure, we eventually decompose the surface input $3g - 3$ pairs of pants. Each pair of pants is a genus zero surface. The algorithmic details can be found in Alg. 1 and 2.

Algorithm 1 Shortest homotopically non-trivial loop

Require: A connected triangle mesh M;
Ensure: The shortest loop γ that is homotopically non-trivial;
  Compute the cut graph Γ of M;
  Prune valence one edges from Γ;
  Slice M along γ to obtain sliced mesh $\bar{M}$;
  $\gamma^* \leftarrow \emptyset$, $L^* \leftarrow \infty$;
  for each $v \in \Gamma$ **do**
    Find the corresponding vertices $v^+, v^- \in \partial\bar{M}$;
    Compute the shortest path γ from v^+ to v^-;
    if $L^* >$ length(γ) **then**
      $\gamma^* \leftarrow \gamma$, $L^* \leftarrow$ length(γ);
    end if
  end for

Algorithm 2 Pants Decomposition

Require: A closed triangle mesh M with genus g;
Ensure: Decompose M into $3g - 3$ pairs of pants;
  updated $\leftarrow$ true;
  while updated **do**
    updated $\leftarrow$ false;
    for each connected component M_i of M **do**
      Compute the shortest loop γ_i of M_i using Alg. 1;
      if γ_i is not empty **then**
        Slice M_i along γ_i;
        updated $\leftarrow$ true
      end if
    end for
  end while

In the following steps, we remesh each surface patch with boundary constraints and eventually glue the remeshed patches together with consistent boundary conditions.

4.3 Conformal Welding Suppose M_1 is a triangle mesh with boundary components, suppose $\gamma_1 \in \partial M_1$. We trace γ_1 to collect an ordered sequence of oriented edges denoted as $\{e_1^1, e_2^1, \ldots, e_n^1\}$. After scaling, we can assume the total length of γ_1 is 2π. We construct a pla-

nar annulus M_2, with exterior boundary γ_2 represented as an ordered sequence of oriented edges $\{e_2^1, e_2^2, \ldots, e_n^2\}$, such that the length of e_k^1 equals to the length of e_k^2. The inner boundary loop is on a smaller circle centered at the origin with radius δ, $0 < \delta < 1$. We use Delaunay refinement algorithm to generate a high quality triangulation of the interior of the annulus to obtain the triangle mesh M_2. We glue M_1 with M_2, such that e_k^1 is glued with e_k^2 isometrically, the union is denoted as M. Please note that the vertex positions of M is not well defined. Suppose $v_k^1 \in \gamma_1$ corresponding to $v_k^2 \in \gamma_2$, they have different coordinates in M_1 and M_2 respectively. However, the edge lengths on M are well defined. The discrete surface Ricci flow only requires the edge lengths, hence M is appropriate for our purpose. The algorithmic details can be found in Alg. 3.

Algorithm 3 Conformal Welding

Require: A triangle mesh M_1 with a boundary component γ_1;

Ensure: M_1 is glued with a planar annulus M_2;

Trace γ_1 to obtain an ordered sequence of oriented edges $e_1^1, e_2^1, \ldots, e_n^1$;

Normalize M_1 such that the total length of γ_1 is 1;

Decompose the unit circle γ_2 to $e_1^2, e_2^2, \ldots, e_n^2$, such that the arc length of e_k^2 equals to the length of e_k^1;

Construct an inner circle γ_3 centered at the origin with radius $\delta < 1$;

Generate a planar triangulation bounded by γ_2 and γ_3 using Delaunay refinement algorithm to obtain a triangle mesh M_2;

Glue M_1 and M_2 by identifying $e_k^1 \in \gamma_1$ and $e_k^2 \in \gamma_2$, the result mesh is M with well defined edge length;

return the welded triangle mesh M.

4.4 Discrete Uniformization First, we compute the discrete conformal metric by setting the target curvature satisfying the Gauss-Bonnet condition. The target curvatures for interior vertices are zeros. Suppose $\partial M = \gamma_0 - \gamma_1 - \cdots - \gamma_n$, for an interior boundary component γ_i with n_i vertices, we set the target curvature for each vertex on γ_i as $-2\pi/n_i$. For the exterior boundary component γ_0 with n_0 vertices, we set the target vertex on γ_0 as $2\pi/n_0$, this will ensure the planar image of M is a convex domain with inner holes. We use Alg. 4 to compute the desired metric.

Once the target metric is obtained, we can isometrically embed the whole mesh on the plane face by face.

4.5 Planar Delaunay Refinement The input object is a two-dimensional polygonal domain Ω, possibly with holes and constraining edges and vertices inside the domain. The *boundary* $\partial\Omega$ is a set of vertices and edges which separates the interior of Ω from its exterior. $\partial\Omega$ is a planar straight line graph (PSLG). We want to generate a mesh $\mathcal{T}$ of Ω, such that $\mathcal{T}$ contains good quality triangles. In order to obtain a good quality mesh, it is necessary for $\mathcal{T}$ to include additional points, called *Steiner points*, vertices of the mesh that are not vertices of the input PSLG. We want the total number of Steiner points to be as small as possible.

Algorithm 4 Discrete Surface Ricci Flow

Require: Triangle mesh M, target curvature $\bar{K}$

Ensure: Discrete Conformal Factor λ

Initialize $\lambda_i \leftarrow 0$, for all $v_i \in V$

while true **do**

Update edge length using vertex scaling Eqn. (3.5)

Update triangulation to be Delauny by edge flips

Update corner angles using Eqn. (3.2)

Update vertex curvature using Eqn. (3.4)

if $\max |\bar{K}_i - K_i| < \varepsilon$ **then**

Return λ

end if

Compute the gradient $\nabla E = (\bar{K}_i - K_i)$

Compute the Hessian matrix H Eqn. (3.8)

Solve linear system $H\mu = \nabla E$

Update the conformal factor $\lambda \leftarrow \lambda - \mu$

end while

Various approaches have been developed for this purpose, such as advancing-front methods, quadtree methods, Delaunay-based methods, [4, 21], and the combinations of them. Most of them work well in practice but come with no guarantee on the quality and size of the generated mesh. The algorithm we use is Delaunay refinement proposed by Chew [4] and Ruppert [21]. It is a simple technique to incrementally placing Steiner points at the circumcenters of bad-quality Delaunay triangles.

A circumcenter of a triangle may lie outside the domain. When it happens, at least a boundary edge (segment) is very close to some existing vertices. Call a vertex *encroaches upon* a segment if it lies inside its diametrical circumcircle. The algorithic details is given in the Alg. 5.

5 Experimental Results

All algorithms have been developed using generic C++ under Visual Studio 2022 on the Windows platform. All the experiments are conducted on a laptop with Intel(R) Core(TM) i7-10750H CPU @2.60GHz with 6 cores and 64GB of memory.

We have tested our proposed method in real car

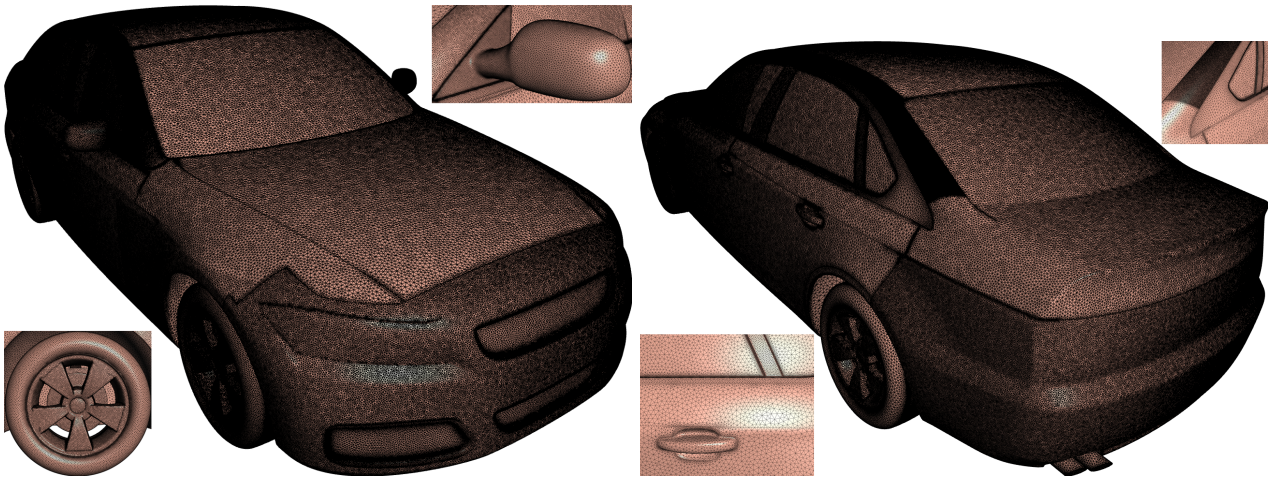

Figure 4: The whole remeshed car model. Left: front view, right: back view.

Algorithm 5 Delaunay Refinement $(\Omega, \theta_{\min})$

Require: A 2d polygonal domain Ω; the desired minimal angle of output triangles $\theta_{\min}$
Ensure: A mesh $\mathcal{T}$ of Ω
  Construct an initial Delaunay mesh $\mathcal{T}$ of $\partial\Omega$;
  while $\exists \tau \in \mathcal{T}$ and MinAngle$(\tau) > \theta_{\min}$ **do**
    let c be the circumcenter of τ;
    if c encroaches upon any segment of $\mathcal{T}$ **then**
      split an encroached segment;
    else
      insert c into the Delaunay mesh $\mathcal{T}$;
    end if
  end while

models for fluid dynamics simulation. As shown in Fig. 4, the initial CAD model is converted to a triangle mesh, after hole filling, defeaturing and other preprocessing steps, the input mesh is a water-tight manifold with $15,013k$ faces. By surface remeshing, the surface triangulation quality has been improved prominently and the number of faces is reduced to $3,398k$. As shown in Fig. 4, the sampling density is adapted to the geometry of the model and the requirement of the simulation. For example, the back surface of the mirror is highly curved, hence the sampling is denser. The triangulations of regions of the body fascia front, the handles and the wheel rims are refined since they are more important for CFD simulation. Experiments show that with the same level of accuracy, the number of cells in the tetrahedral final mesh is reduced by 43.56%, and the volumetric mesh generation is 3.29 times faster, the CFD simulation is 3.47 times faster.

Fig. 5 shows the topological and geometric complexities of the car model. Some mechanical parts have very high genus, and some geometric structures are highly refined and almost self-intersecting. Our proposed algorithm can partition high genus surfaces into poly-annuli automatically, preserve sharp geometric features, and avoid self-intersections.

Fig. 7 shows parts of the suspension system: in the first row, the left frame displays the original model and the right frame shows the planar image of the welded surface under the conformal mapping; in the second row, the right frame shows the planar image of the model with the welded annulus removed, the left frame demonstrates the conformality of the mapping by checkerboard texture mapping; the third row compares the initial low mesh quality (left frame) and the high mesh quality of the remeshing result (right frame). Similarly, Fig. 8 and Fig. 6 show the remeshing process of the radiator shell and part of the chassis (of a different car) respectively.

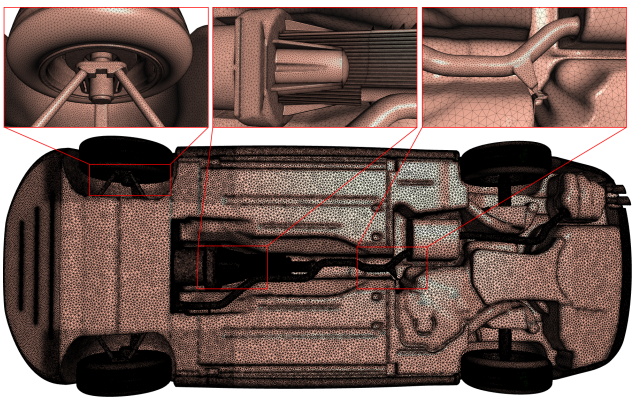

Figure 5: The remeshed car model (the bottom view).

Fig. 9 demonstrates a challenging case. The genus of the input brake surface is 83, the conventional surface segmentation algorithm will decompose it input 246 pairs of pants, and each patch is relatively small, hence the whole processing in inefficient. In this case, we compute the mid-plane of the model, which cut through all the handles and divide the surface into two halves, each half is a genus zero surface with 84 boundary components. The dynamic Ricci flow combined with the conformal welding technique can handle this type of poly-annulus without any difficulty. The first row right frame shows the image of conformal parameterization of the welded model. The second row right frame shows the planar image of the brake model only, the left frame shows the conformality of the mapping by checkerboard texture mapping. The third row compares the original meshing (left frame) and the remeshed result (right frame). This example shows the proposed method can handle surfaces with complicated topologies.

Table 1 summarizes the statistics of our experiments. We selected some representative mechanical parts of the car body, and give the running time for conformal parameterization step and the remeshing step. The table also gives the comparison between the geometric complexity of the original mesh and the remeshed mesh in terms of the numbers of vertices and faces.

Finally, we evaluate the mesh quality based on angles and skewness. The skewness here refers to the measure of the deformation of individual triangles in a mesh. In general, low skewness values indicate well-shaped elements that are closer to ideal shapes, while high skewness values suggest distorted elements.

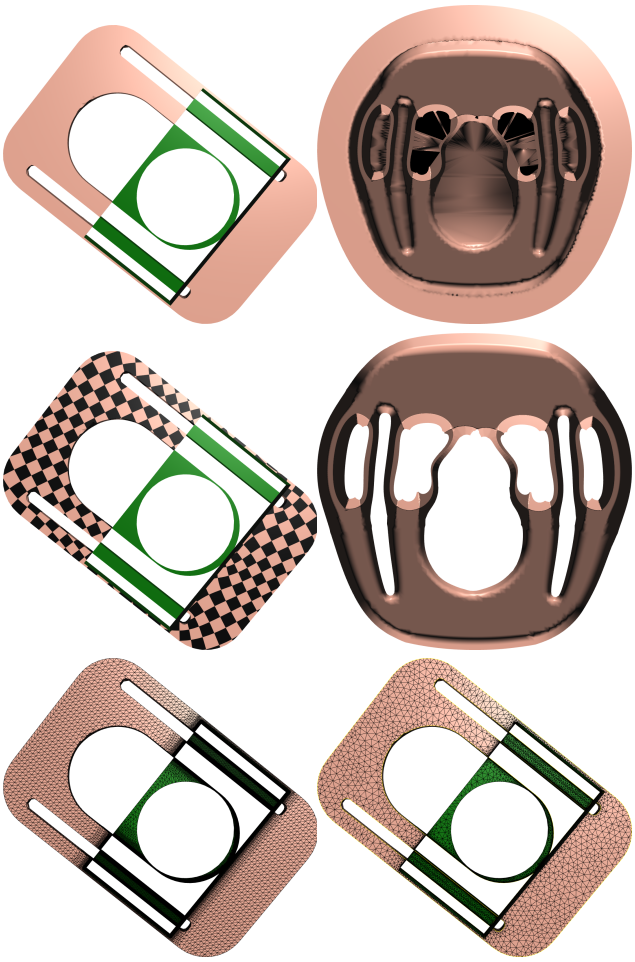

Figure 7: The car suspension part.

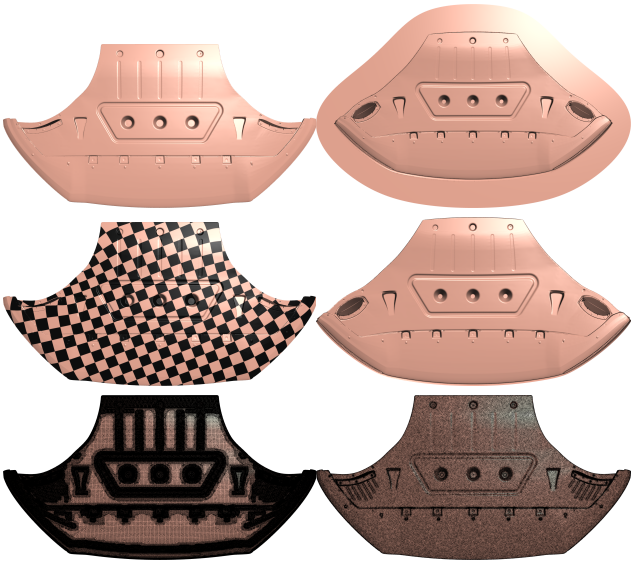

Figure 6: One part of the car chassis.

Model	#Vertices	#Faces	Param.	Remesh
Suspension 7	87k/23k	173k/43k	3m40s	6s
Shield 2	134k/59k	263k/113k	6m39s	18s
Shell 8	263k/69k	524k/137k	8m15s	36s
Chassis 6	338k/81k	673k/158k	11m21s	25s
Brake 9	804k/175k	1572k/315k	34m48s	5m31s

Table 1: Runtimes of the parameterization step and remeshing step on the selective parts of a car model, the numbers before and after slash represent the numbers of the cells in original model and remeshed model respectively.

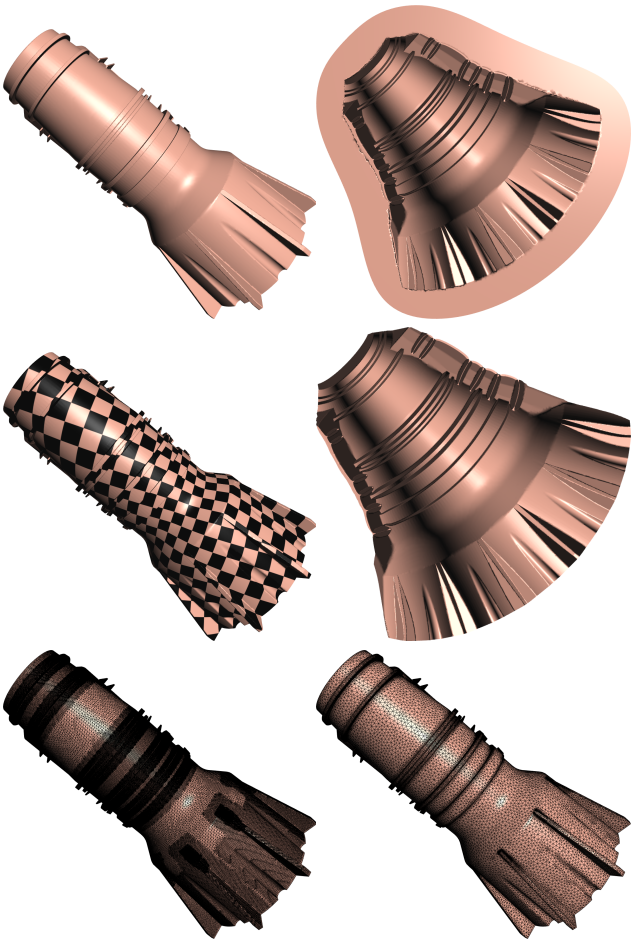

Figure 8: One part of the radiator shell.

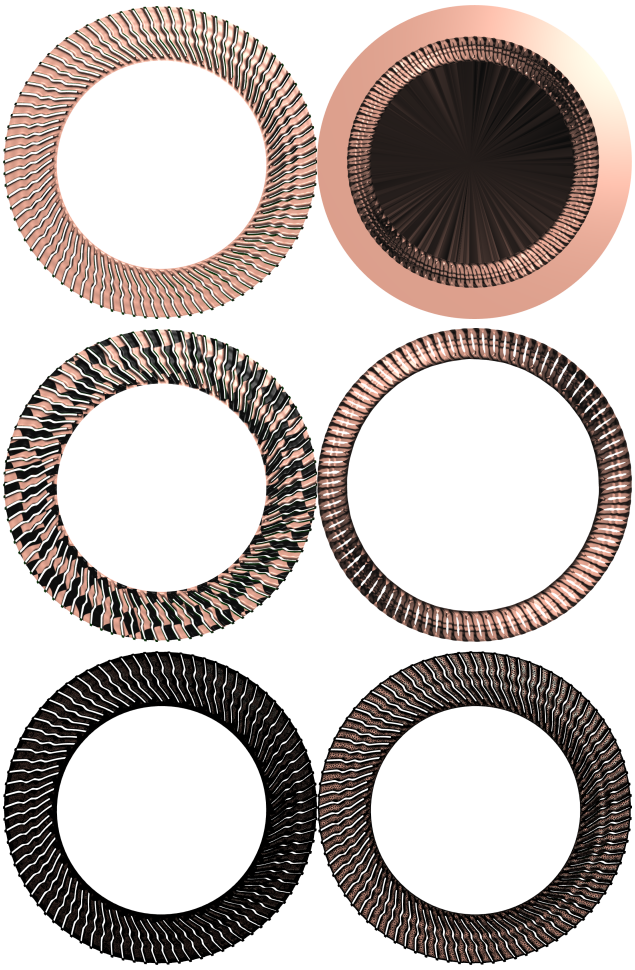

Figure 9: The brake block of the car.

Fig. 10 displays a histogram illustrating mesh quality in terms of angles and skewness of the original and remeshed car models. The vertical axis represents the proportion rather than the quantity, offering a quantitative insight into the distribution. The remeshed mesh exhibits superior quality compared to the original mesh, characterized by a higher concentration of angles near 60 degrees and a greater prevalence of triangles approaching the ideal regular triangle.

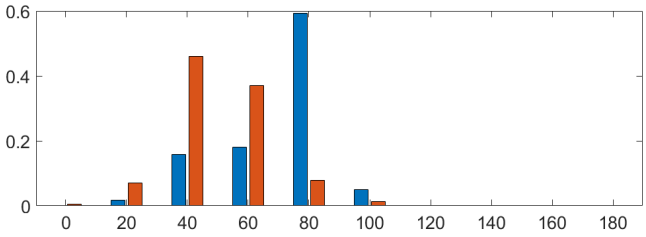

(a). angle evaluation

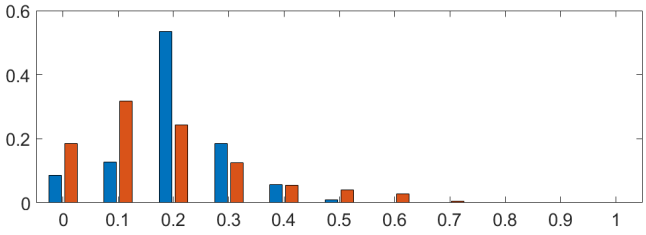

(b). skewness evaluation

Figure 10: The comparison of mesh quality before and after remeshing for the car model. Blue: the result of original surface; Orange: the result of remeshing result.

6 Conclusion

This work proposal a practical algorithm to improve the robustness of surface remeshing based on conformal welding technique. The input surface is a topological annulus, it is welded with a topological cylinder along one of its boundary component, and flattened onto a convex planar domain. This guarantees the conformal parameterization of the input surface is an embedding, so that the planar image can be triangulated using classical planar Delaunay refinement algorithm, the planar triangulation is pulled back to the original surface to produce high quality surface triangulation. Our experiments on real car models demonstrate the effectiveness of the proposed method.

In the future, we will explore further to generalize the method to surfaces with more complicated topologies.

Acknowledgement

This research was supported by the National Natural Science Foundation of China T2225012, 61936002, National Institutes of Health grant #R21EB029733 and National Science Foundation grant #2213852.

References

[1] Alliez, P., Desbrun, M.: Progressive meshes. In: Proceedings of the 28th Annual Conference on Computer Graphics and Interactive Techniques. pp. 99–108 (2001)

[2] Berg, M.d., Cheong, O., Kreveld, M.v., Overmars, M.: Computational Geometry: Algorithms and Applications. Springer-Verlag TELOS, Santa Clara, CA, USA, 3rd ed. edn. (2008)

[3] Cheng, S.W., Dey, T.K., Shewchuk, J.R.: Delaunay Mesh Generation. CRC Press (2010)

[4] Chew, L.P.: Guaranteed-quality triangular meshes. Tech. Rep. TR 89-983, Dept. of Comp. Sci., Cornell University (1989)

[5] Chow, B.: The Ricci flow on the 2-sphere. J. Differential Geom. **33**(2), 325–334 (1991)

[6] Du, Q., Faber, V., Gunzburger, M.: Centroidal voronoi tessellations: Applications and algorithms. SIAM Review **41**, 637–676 (1999)

[7] Edelsbrunner, H., Harer, J.L.: Computational Topology: An Introduction. American Mathematical Society (2010)

[8] Garland, M., Heckbert, P.S.: Surface simplification using quadric error metrics. In: Proceedings of the 24th Annual Conference on Computer Graphics and Interactive Techniques. pp. 209–216 (1997)

[9] Gary P. T. Choi, Yusan Leung-Liu, X.G., Lui, L.M.: Parallelizable global conformal parameterization of simply-connected surfaces via partial welding. SIAM Imaging Sciences **13**(3), 1049–1083 (2010)

[10] Gu, X., Guo, R., Luo, F., Sun, J., Wu, T.: A discrete uniformization theorem for polyhedral surfaces i. Journal of Differential Geometry (JDG) **109**(3), 431–466 (2018)

[11] Gu, X., Luo, F., Sun, J., Wu, T.: A discrete uniformization theorem for polyhedral surfaces i. Journal of Differential Geometry (JDG) **109**(2), 223–256 (2018)

[12] Gu, X., Yau, S.T.: Computational Conformal Geometry, Advanced Lectures in Mathematics, vol. 3. International Press and Higher Education Press (2007)

[13] Gu, X., Yau, S.T.: Computational Conformal Geometry. International Press and Higher Education Press (2020)

[14] Hamilton, R.: The Ricci Flow on Surfaces. A.M.S. Contemp. Math. **71**(1), 237–261 (1986)

[15] Hang Si, N.L., Gu, X.: Surface remeshing based on conformal uniformization. In: Proceedings of the SIAM International Meshing Roundtable 23 (2023)

[16] Kazhdan, M., Bolitho, M., Hoppe, H.: Poisson surface reconstruction. In: Proceedings of the fourth Eurographics symposium on Geometry processing. pp. 61–70 (2006)

[17] Lok Ming Lui, Wei Zeng, S.T.Y., Gu, X.: Shape analysis of planar multiply-connected objects using conformal welding. IEEE Transactions on Pattern Analysis and Machine Intelligence (IEEE TPAMI) **36**(7), 1384–1401 (2013)

[18] Perelman, G.: The entropy formula for the ricci flow and its geometric applications (2002). https://doi.org/10.48550/ARXIV.MATH/0211159, `https://arxiv.org/abs/math/0211159`

[19] Perelman, G.: Ricci flow with

surgery on three-manifolds (2003). https://doi.org/10.48550/ARXIV.MATH/0303109, https://arxiv.org/abs/math/0303109

[20] Peyré, J., Oudot, S., Keriven, R., Cohen-Steiner, D.: Cgal: Computational geometry algorithms library. ACM Transactions on Mathematical Software (TOMS) **46**(3), 1–27 (2020)

[21] Ruppert, J.: A Delaunay refinement algorithm for quality 2-dimensional mesh generation. Journal of Algorithms **18**(3), 548–585 (1995)

[22] Shewchuk, J.R.: Triangle: Engineering a 2d quality mesh generator and delaunay triangulator. In: Applied Computational Geometry: Towards Geometric Engineering. pp. 203–222 (1996)